

Influence of surface roughness on the optical properties of plasmonic nanoparticles

Andreas Trügler, Jean-Claude Tinguely, Joachim R. Krenn, Andreas Hohenau, and Ulrich Hohenester*

Institut für Physik, Karl-Franzens-Universität Graz, Universitätsplatz 5, 8010 Graz, Austria

(Dated: September 28, 2018)

For plasmonic nanoparticles, we investigate the influence of surface roughness inherent to top-down fabrication on the optical properties, and find that it has a surprisingly small influence on the position and width of the plasmon peaks. Our experimental observation is supported by simulations based on the boundary element method approach. Using a perturbation approach, suitable for metallic nanoparticles with a moderate degree of surface roughness, we demonstrate that the reason for this lies in *motional narrowing* where the plasmon averages over the random height fluctuations. Surface roughness in large arrays of identical nanoparticles, such as encountered in the context of metamaterials, is thus expected to not constitute a major roadblock.

PACS numbers: 73.20.Mf, 78.67.Bf, 03.50.De

Plasmonics bridges the gap between the micrometer length scale of light and the length scale of nanostructures.¹ This is achieved by binding light to coherent charge density oscillations of metallic nanostructures, so-called surface plasmons, which allow to focus electromagnetic radiation down to spots with spatial dimensions of the order of a few nanometers.² Coupling of quantum emitters, such as quantum dots or molecules, with plasmonic nanostructures can strongly modify their excitation and emission properties, observable in fluorescence³ or surface enhanced Raman scattering,⁴ and offers a unique means for tailoring light-matter interaction at the nanoscale. This has found widespread applications ranging from (bio)sensors⁵ and solar cells⁶ to optical and quantum communication technology.⁷ Plasmonic nanoparticles are also at the heart of the emerging fields of metamaterials and optical cloaking.⁸

Huge advances in fabrication techniques over the last years allow nowadays to fabricate plasmonic nanostructures with well understood and predictable properties. Nevertheless, practically all metallic nanoparticles suffer from size inhomogeneities and nanoscale surface roughness,^{9,10} which results in deviations of the plasmonic properties from those of idealized nanoparticles.¹¹ Particularly top-down approaches for nanoparticle fabrication often involve vacuum deposition of the metal structures, which leads to polycrystalline particles with an apparent surface roughness.¹⁰ Despite the important role of surface roughness, there is still little understanding about the impact of such imperfection on the optical properties. Recent publications report on the control of nanoscale roughness and its strong effect on the nanoparticles far- and near-field optical properties.^{9,10,12} However, varying surface roughness is often accompanied by varying crystallinity, and therefore the results do not allow for a clear distinction between the contributions of the surface and the bulk.

In this paper we provide evidence from experiment, theory, and simulation that a moderate amount of surface roughness has no significant impact on the far-field optical properties of metallic nanoparticles. We interpret this as a kind of *motional narrowing*, where the surface

plasmon averages over the random height fluctuations of the metal surface, which leads to destructive interference and an overall small net effect. Our findings might be beneficial for the design of metamaterials, which rely on large ensembles of practically identical particles, as well as devices based on the far-field properties of plasmonic nanoparticles.

Experiment.—We measured the scattering spectra of individual polycrystalline (rough) gold nanoparticles to probe the influence of unavoidable surface roughness on the plasmonic signature of nanoparticles of nominally identical shape. The particles were fabricated by electron beam lithography on an indium-tin oxide (ITO) covered glass substrate. The substrate was coated with a polymer resist, which was then exposed and chemically developed. Vacuum deposition of gold and a liftoff process lead to polycrystalline particles (crystallite size ~ 20 nm) of designed shapes,¹³ but with apparent surface roughness, as shown in Fig. 1(c). The particles were probed in a dark field microscope, collecting the scattered light by a $40\times$, 0.75 numerical aperture objective and analyzing it with a spectrograph.

Fig. 1(a) shows exemplarily scattering spectra of four individual 50 nm wide, 100 nm long, and 45 nm high gold nanorods. Although the exact particle shapes differ due to nanoscale roughness [Fig. 1(c)], the dipolar plasmon resonance positions and the spectral widths of the four particles under consideration differ less than 20% of the full width at half maximum. Similar results were also observed for other nanoparticles shapes (not shown). From this we conclude that surface roughness has a surprisingly small influence on the optical properties of plasmonic nanoparticles, at least in the regime where the roughness does not lead to a noticeable change of the particle aspect ratio.

Simulation.—We additionally performed simulations based on the boundary element method (BEM),^{15–18} using a dielectric function representative for gold¹⁴ and an effective refractive index of $n_b = 1.65$ for the ITO covered glass substrate. The particle shapes in the (x, y) -plane were extracted from the SEM images [Fig. 1(c)]. We use a particle height of 45 nm and round off the edges

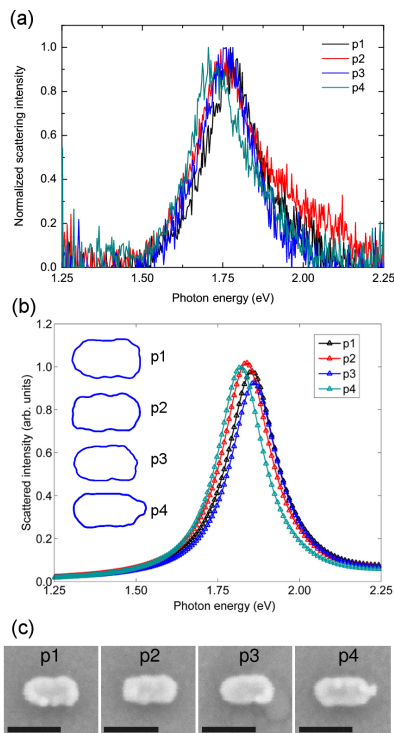


FIG. 1: (color online) (a) Scattering spectra of four individual gold nanorods excited with a polarization parallel to the particles long axis. Since the repeatability of the scattering intensity is only within $\sim 20\%$, the spectra are normalized to facilitate the spectral comparison. (b) Spectra simulated within our BEM approach, using the gold dielectric function of Ref. 14 and a refractive index of $n_b = 1.65$ for the substrate, for the particle shapes extracted from the SEM images reported in panel (c). The particle height is 45 nm. The lengths of the scalebars in the lower panels are 100 nm.

with a curvature radius of 5 nm. The simulated scattering spectra are reported in Fig. 1(b). In accordance to experiment, we find a surprisingly small influence of the roughness-related particle shape on the plasmon peak positions. Also the absolute peak heights vary by less than 5 percent. We note that there are small differences between experiment and theory, such as the weak shoulder around 2 eV, but the overall agreement regarding both peak positions and widths is striking.

The agreement between the measured and calculated widths of the plasmon peaks is quite remarkable since in our simulations we do not consider plasmon dephasing due to surface roughness scatterings, but only include electrodynamic decay channels. From supplementary calculations we find that the absorption cross sections are about three times larger than the scattering cross sections. Thus, ohmic losses (described through the imaginary part of the dielectric function) dominate over radiative damping as well as over dephasing losses due to surface roughness scatterings. For smaller particle sizes, comparable to the electron mean free path of several nanometers, such dephasing will become increas-

ingly important and could no longer be neglected in the simulations.

To inquire into the reasons for the almost negligible influence of surface roughness on the plasmon peak positions, in the following we use cylindrical nanorods as a showcase system, because of their extreme sensitivity to variations of the dielectric environment and shape.¹⁹ We also employ the quasistatic approximation,^{15,21} which is justified for small particles and will allow us further below to introduce a perturbation analysis. With respect to the retarded BEM simulations, the quasistatic approximation is expected to lead to a slight overestimation of the plasmon peak energy.

In our simulations we model surface roughness by adding stochastic height variations to the smooth surface of an ideal nanoparticle. In two dimensions and for a box with periodic boundary conditions, height variations with a Gaussian autocorrelation can be obtained by attaching to all Fourier coefficients arbitrary phase factors $e^{i\phi_{\text{rnd}}}$ viz.

$$h(x, y) = \Delta h \Re \left[\mathcal{F}^{-1} \left(e^{-\frac{1}{2}\sigma_h^2(k_x^2 + k_y^2) + i\phi_{\text{rnd}}} \right) - \frac{1}{2} \right], \quad (1)$$

where \mathcal{F}^{-1} denotes the inverse Fourier transform and σ_h^2 is the variance of the height fluctuations. We next map $h(x, y)$ to the nanoparticle surface and displace the vertices of the nanoparticle along the surface normal directions.²² A typical realization of surface roughness is depicted in Fig. 2(b) for a nanorod.

Figure 2(a) shows spectra for gold nanorods for different height-to-diameter ratios. Throughout we set the rod diameter to 30 nm and use $\sigma_h = 3$ nm. For each spectrum we average over hundred random realizations of surface roughness and assume light excitation with a polarization along long axis of the rod. One clearly observes that when increasing the amount of surface roughness, by choosing different values of Δh , the shape of the averaged spectra does not change (with exception of an overall small red shift). Only the variance of the individual spectra increases with increasing Δh , as indicated by the error bars. Thus, our numerical simulations demonstrate that *surface roughness has a surprisingly small influence on the optical properties of plasmonic nanoparticles*.

Things change considerably if we use the more regular height variations of a rippled rod, depicted in Fig. 2, that were recently suggested as a viable model for surface roughness.²⁰ Here the spectra strongly shift to the red when Δh is increased, as depicted by the gray lines on the left of Fig. 2. Thus, it appears that the irregular shape of the surface height fluctuations is responsible for the overall small shift of the plasmon peak position. Indeed, when ripples are introduced not only along the symmetry axis of the nanorod but also around its circumference (here 6 ripples) the redshift becomes strongly reduced, as shown by the dashed gray lines.

Theory.—We next develop a perturbation analysis which will help us to understand the effects of surface roughness more deeply. Let us first recall the basic ele-

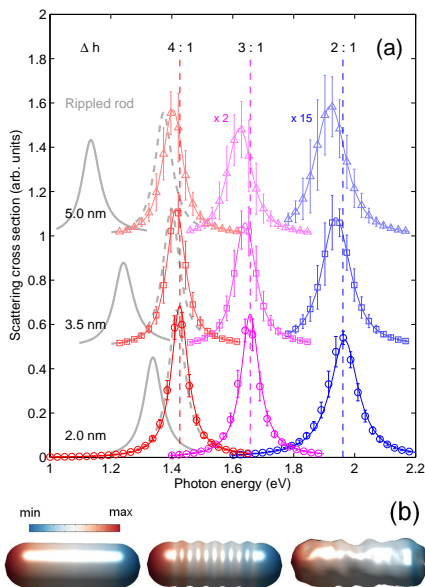


FIG. 2: (color online) (a) Simulated spectra for nanorods with a diameter of 30 nm and for height-to-diameter ratios of 2 : 1, 3 : 1, and 4 : 1. In our simulations we use a dielectric function representative for gold¹⁴ and a homogeneous dielectric background ($n_b = 1.5$), and add stochastically surface roughness according to the prescription of Eq. (1) with $\sigma_h = 3$ nm and for different Δh values, which determine the height variations of surface roughness. Each spectrum is averaged over 100 randomly generated nanoparticles. The solid lines report the spectra of the smooth nanorods in the panel for $\Delta h = 2$ nm, and the mean values of the spectra otherwise. The gray lines report results for rippled rods, as discussed in the text. The spectra for ratios 2 : 1 and 3 : 1 have been magnified by factors of 15 and 2, respectively. (b) Surface charge distributions σ_a for the optically active plasmon modes for the smooth (left), rippled (middle), and rough (right) nanorods.

ments of the BEM approach. For a metallic nanoparticle with dielectric function $\epsilon_m(\omega)$ embedded in a dielectric background with constant ϵ_b , the solutions of the Poisson equation within the two media are given by the Green function $G(\mathbf{r}, \mathbf{r}') = 1/|\mathbf{r} - \mathbf{r}'|$. The electrostatic potential can be written in the ad-hoc form $\phi = \langle G, \sigma \rangle + \phi_{\text{ext}}$,¹⁵ where σ is a surface charge distribution located at the boundary ∂V of the metallic nanoparticle, which has to be chosen such that the boundary conditions of Maxwell's equations are fulfilled, $\langle G, \sigma \rangle = \int_{\partial V} G(\mathbf{r}, \mathbf{s}) \sigma(\mathbf{s}) d\mathbf{s}$ defines an inner product, and ϕ_{ext} is the potential of the external perturbation.

Continuity of the normal component of the dielectric displacement at the metal-dielectric interface gives an expression

$$\Lambda(\omega)\sigma + \left\langle \frac{\partial G}{\partial \hat{n}}, \sigma \right\rangle = -\frac{\partial \phi_{\text{ext}}}{\partial \hat{n}}, \quad \Lambda = 2\pi \frac{\epsilon_m + \epsilon_b}{\epsilon_m - \epsilon_b} \quad (2)$$

that can be used for the calculation of the surface charge distribution. Here $\partial G / \partial \hat{n} \equiv F$ and $\partial \phi_{\text{ext}} / \partial \hat{n} \equiv \phi'_{\text{ext}}$ denote the surface derivatives of the Green function and

the external potential, respectively.

We next define the right and left eigenvectors σ_k and $\tilde{\sigma}_k$ of the surface derivative of the Green function through^{21,23}

$$\langle F, \sigma_k \rangle = \lambda_k \sigma_k, \quad \langle \tilde{\sigma}_k, F \rangle = \lambda_k \tilde{\sigma}_k, \quad (3)$$

which form a biorthogonal set with $\langle \tilde{\sigma}_k, \sigma_{k'} \rangle = \delta_{kk'}$. The functions σ_k can be interpreted as the surface plasmon *eigenmodes*, and the response to any external perturbation can be decomposed into these modes viz.

$$\sigma = -\sum_k \frac{\sigma_k}{\Lambda(\omega) + \lambda_k} \langle \tilde{\sigma}_k, \phi'_{\text{ext}} \rangle. \quad (4)$$

Apparently, a given mode k gives a noticeable contribution only if the coupling $\langle \tilde{\sigma}_k, \phi'_{\text{ext}} \rangle$ to the external potential (in our case plane wave illumination) is sufficiently strong and if the denominator becomes small. The plasmon resonance condition translates to $\text{Re}[\Lambda(\omega) + \lambda_k] = 0$, when assuming that the imaginary part of ϵ has an only weak frequency dependence. This is an extremely useful expression as it allows to separate the structural properties (described by λ_k) from the material properties (described by Λ).

We are now in the position to analyze the effects of a moderate surface roughness, which we model as a distortion of the surface ∂V from its ideal shape. In turn, the surface derivative of the Green function F changes to $F + \delta F$, where δF is expected to have the same random character as the surface fluctuations.²⁴ How does λ_k , which determines the peak positions of the plasmons, change in case of surface roughness? When δF is sufficiently small we can employ perturbation theory, in complete analogy to quantum mechanics. We treat F as the unperturbed part and δF as the ‘‘perturbation’’. Following Ref. 25 we introduce for a given plasmon mode a the projector

$$\frac{Q_0}{a} \equiv \sum_{k \neq a} \frac{\sigma_k^0 \tilde{\sigma}_k^0}{\lambda_a^0 - \lambda_k^0}, \quad (5)$$

where the superscript 0 indicates the eigenvalues and eigenfunctions for the ideal nanoparticle surface. The corrections to λ_a then become within lowest order perturbation theory

$$\lambda_a^1 = \left\langle \tilde{\sigma}_a^0, \delta F \sigma_a^0 \right\rangle \quad (6a)$$

$$\lambda_a^2 = \left\langle \tilde{\sigma}_a^0, \delta F \frac{Q_0}{a} \delta F \sigma_a^0 \right\rangle. \quad (6b)$$

From this we can draw an important conclusion for the dipolar modes, whose σ_a^0 distributions usually vary smoothly on the length scale of surface roughness. Since Eq. (6a) averages the random variations δF over the unperturbed distributions σ_a^0 , the positive and negative δF values associated with the height variations of surface roughness will become effectively averaged out. This results in a small λ_a^1 correction, and consequently *surface*

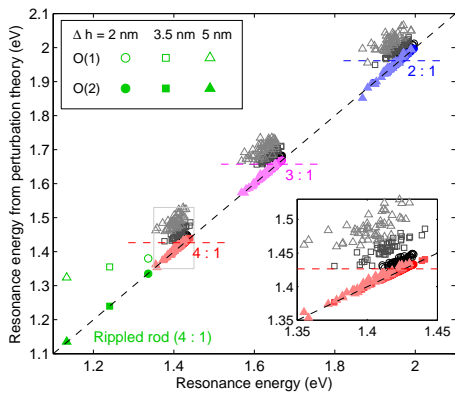


FIG. 3: (color online) Comparison of full simulations and perturbation theory of Eq. (6), for the positions of the resonance energies of the optically active surface plasmon modes with polarization along the long axis of the rod. The open and filled symbols report results obtained within first and second order perturbation theory, respectively. In the inset we show a blow-up for the nanorod with a height-to-diameter ratio of 4 : 1.

roughness does not affect significantly the optically active plasmon modes.

In a sense, this finding is similar to motional narrowing in semiconductor quantum wells,²⁶ where the motion of an optically excited electron-hole pair (exciton) is subject to the potential induced by the local monolayer fluctuation inherent to quantum wells. When the exciton propagates through the well it “averages” over the fluctuations of the random potential, which results in a narrowing of the exciton lineshape.

In Fig. 3 we compare the results of our full simulations with the predictions of Eq. (6). The open and full symbols show the true resonance energies (obtained from

$\text{Re}[\Lambda(\omega) + \lambda_k] = 0$) and the perturbation results (obtained with $\lambda_a^0 + \lambda_a^1$ and $\lambda_a^0 + \lambda_a^1 + \lambda_a^2$, respectively). Symbols on the diagonal correspond to the situation where perturbation theory and the full BEM simulations coincide. In all cases the shift of the resonance with respect to the positions of the smooth nanorod (dashed horizontal lines) is small. Quite generally, first order perturbation theory, which ignores any variations of the surface charge distribution ($\sigma_a = \sigma_a^0$), leads to a blue shift. Only for second order perturbation theory, which includes modification of σ_a , the red shift of the plasmonic resonances is properly reproduced.

As for the rippled rod, we observe that the first-order corrections λ_a^1 are small. This is because the argument of motional narrowing in principle also applies here. However, through the admixture of excited surface plasmon modes σ^0 , described by the second-order correction λ_a^2 , the surface plasmon can accommodate to the regular height variations of the rippled rod, and the plasmon peak position becomes strongly red-shifted. No corresponding conclusions prevail for the stochastic height variations.

Summary.—In summary, we have investigated the influence of surface roughness on the optical properties of plasmonic nanoparticles, and have found a surprisingly small effect. Using a simulation and perturbation theory approach, we have been able to trace back our findings to a motional narrowing, where the plasmon averages over the random height fluctuations. As no corresponding conclusions prevail for the near-field optical properties, our results are in accordance with the findings of “hot spots” in fluorescence or surface enhanced Raman scattering experiments.

This work has been supported in part by the Austrian science fund FWF under project No. P21235-N20.

* Electronic address: ulrich.hohenester@uni-graz.at

¹ S. A. Maier, *Plasmonics: Fundamentals and Applications* (Springer, Berlin, 2007).

² J. A. Schuller, E. S. Barnard, W. Cai, Y. C. Jun, J. S. White, and M. L. Brongersma, *Nature Materials* **9**, 193 (2010).

³ P. Anger, P. Bharadwaj, and L. Novotny, *Phys. Rev. Lett.* **96**, 113002 (2006).

⁴ K. Kneipp, M. Moskovits, and H. Kneipp, eds., *Surface-Enhanced Raman Scattering*, vol. 103 of *Topics in Applied Physics* (Springer, Heidelberg, New York, 2006).

⁵ J. N. Anker, W. P. Hall, O. Lyandres, N. C. Shah, J. Zhao, and R. P. V. Duyne, *Nature Mater.* **7**, 442 (2008).

⁶ V. E. Ferry, L. A. Sweatlock, D. Pacifici, and H. A. Atwater, *Nano Lett.* **8**, 4391 (2008).

⁷ D. E. Chang, A. S. Sorensen, P. R. Hemmer, and M. D. Lukin, *Phys. Rev. Lett.* **97**, 053002 (2006).

⁸ J. B. Pendry, D. Schurig, and D. R. Smith, *Science* **312**, 1780 (2006).

⁹ J. Rodriguez-Fernandez, A. M. Funston, J. Perez-Juste,

R. A. Alvarez-Puebla, L. M. Liz-Marzan, and P. Mulvaney, *Phys. Chem. Chem. Phys.* **11**, 5909 (2009).

¹⁰ K.-P. Chen, V. P. Drachev, J. D. Borneman, A. V. Kildishev, and V. M. Shalaev, *Nano Letters* p. 916 (2009).

¹¹ W. L. Barnes, *J. Opt. A* **11**, 114002 (2009).

¹² J. S. Huang, V. Callegari, P. Geisler, C. Brünig, J. Kern, J. Prangnsma, P. Weinmann, M. Kamp, A. Forchel, P. Biagioni, et al., arXiv:1004.1961 (2010).

¹³ A. Hohenau, H. Ditlbacher, B. Lamprecht, J. R. Krenn, A. Leitner, and F. R. Aussenegg, *Microelec. Engin.* **83**, 1464 (2006).

¹⁴ P. B. Johnson and R. W. Christy, *Phys. Rev. B* **6**, 4370 (1972).

¹⁵ F. J. Garcia de Abajo and A. Howie, *Phys. Rev. B* **65**, 115418 (2002).

¹⁶ U. Hohenester and J. R. Krenn, *Phys. Rev. B* **72**, 195429 (2005).

¹⁷ U. Hohenester and A. Trügler, *IEEE J. of Selected Topics in Quantum Electronics* **14**, 1430 (2008).

¹⁸ F. J. G. de Abajo, *Rev. Mod. Phys.* **82**, 209 (2010).

- ¹⁹ J. Becker, A. Trügler, A. Jakab, U. Hohenester, and C. Sönnichsen, *Plasmonics* **5**, 161 (2010).
- ²⁰ C. Pecharromás, J. Pérez-Juste, G. Mata-Osoro, L. M. Liz-Marzán, and P. Mulvaney, *Phys. Rev. B* **77**, 035418 (2008).
- ²¹ R. Fuchs, *Phys. Rev. B* **11**, 1732 (1975).
- ²² Mapping can be facilitated by computing $h(x, y, z)$ in three dimensions, with an expression similar to Eq. (1), and interpolating the stochastic height variations h to the nanoparticle surface.
- ²³ I. D. Mayergoyz, Z. Zhang, and G. Miano, *Phys. Rev. Lett.* **98**, 147401 (2007).
- ²⁴ This is because $F(\mathbf{s}, \mathbf{s}')$ is governed for $\mathbf{s} \approx \mathbf{s}'$, where deviations of the ideal shape are most significant, directly by the surface curvature.
- ²⁵ A. Messiah, *Quantum Mechanics* (North-Holland, Amsterdam, 1965).
- ²⁶ M. Z. Maialle, E. A. de Andrada e Silva, and L. J. Sham, *Phys. Rev. B* **47**, 15 776 (1993).